Multifunctional Amine Modifiers for Selective Dehydration of Methyl Lactate to Acrylates

Yutong Pang[1,2], ChoongSze Lee[1],
Bess Vlaisavljevich[2,3], Christopher P. Nicholas[4,5], Paul J. Dauenhauer[1,2,5]*

[1] University of Minnesota, Department of Chemical Engineering & Materials Science, 421 Washington Ave. SE, Minneapolis, MN, USA 55455

[2] Center for Sustainable Polymers, University of Minnesota, 207 Pleasant Street SE, Minneapolis, MN, USA 55455

[3] University of South Dakota, Department of Chemistry, 115 Churchill-Haines Laboratory, 414 E. Clark Street, Vermillion, SD, 57069, USA.

[4] C2P Sciences L3C, 825 Chicago Ave. Suite 10B, Evanston, IL, USA 60202

[5] Låkril Technologies Corporation, 2225 W. Harrison St. Suite 102, Chicago, IL, USA 60612

* Corresponding author: hauer@umn.edu

Abstract. Dehydration of methyl lactate to acrylic acid and methyl acrylate was experimentally evaluated over Na-FAU zeolite catalyst impregnated with multifunctional diamines. 1,2-bis(4-pyridyl)ethane (12BPE) and 4,4′-trimethylenedipyridine (44TMDP), at a nominal loading of 40 wt% or two molecules per Na-FAU supercage, afforded a dehydration selectivity of 96±3% over 2000 min time on stream, exceeding the selectivity target of 90% for commercial viability. During continuous reaction at 300 °C, the amine loadings in Na-FAU remained constant for 12BPE but decreased as much as 83% for 44TMDP. Although 12BPE and 44TMDP have van der Waals diameters approximately 90% of the Na-FAU window opening diameter, both flexible diamines interact with internal active sites of Na-FAU as characterized by infrared spectroscopy. Tuning the weighted hourly space velocity (WHSV) from 0.9 to 0.2 h^{-1} afforded a yield as high as 92% at a selectivity of 96% with 44TMDP impregnated Na-FAU, resulting in the highest yield reported to date.

Introduction. Acrylic acid and its alkyl acrylate derivatives are high production volume chemicals for which a bio-based synthetic route is desirable to provide a sustainable manufacturing process. These derivatives act as major building blocks in industrial and consumer products including adhesives, adsorbents, and coatings.[1,2] Acrylics are currently produced from the oxidation of petroleum-derived propylene by a two-step oxidation via acrolein over bismuth molybdate catalysts.[3] Since most acrylics are manufactured by this process, the global acrylic market size is projected to reach $14 billion USD by 2030 at an annual growth rate of 3-4 %.[4] One alternative pathway to form acrylates is the dehydration of biomass-derived lactic acid or alkyl lactates over solid acid catalysts including inorganic salts,[5–11] hydroxyapatite,[12–14] and zeolites.[15–22] As lactic acid tends to self-polymerize even at room temperature,[23,24] alkyl lactates, including methyl lactate, can serve as a reactant surrogate to prevent reactant oligomerization while preserving all major

reaction pathways. In addition to acrylic acid, methyl acrylate is also the dehydration product from methyl lactate (**Scheme 1**). While dehydration selectivity values as high as 93%[8] and 78%[14] can be achieved over inorganic salts and hydroxyapatite, respectively, due to the low intrinsic catalyst activity, a relatively high temperature above 350 ºC is required to achieve a conversion of at least 70% .[8]

Conversely, the highest dehydration selectivity reported is typically 50-to-70% on metal-exchanged zeolites with almost complete conversion at temperatures as low as 325 ºC. Example zeolite catalysts include alkali metal-exchanged FAU[15,16,18,20,21] and BEA[17,19] zeolites. One recent study demonstrated a selectivity as high as 80% over a potassium-modified ZSM-5 zeolite.[22] However, further improvement in dehydration selectivity above 90% is desired for the commercial viability of lactates to acrylates. In our previous work, methyl lactate was converted to methyl acrylate and acrylic acid at a dehydration selectivity of 61% and a conversion of 92% at 300 ºC over a
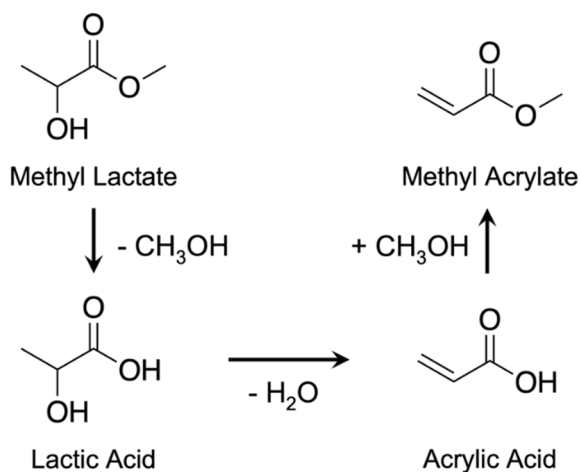
Scheme 1. Methyl lactate is proposed to first undergo hydrolysis to lactic acid and methanol. Lactic acid then undergoes dehydration to acrylic acid, which may further react with methanol from methyl lactate to methyl acrylate.

sodium-exchanged FAU zeolite (Na-FAU, Si:Al = 2.6).[25] Two major reaction pathways were observed over Na-FAU: (i) dehydration to methyl lactate and acrylic acid; (ii) decarbonylation to carbon monoxide, methanol, and acetaldehyde (**Figure 1**). Previous research proposed that dehydration occurs on the sodium acid sites native to the Na-FAU materials, with decarbonylation occurring on the Brønsted acid sites (BAS) generated during the reaction.[26–28]

Cofeeding pyridine as a BAS titrant can suppress decarbonylation and improve dehydration selectivity by 13%.[26,28] Our previous work further investigated the effect of titrant basicity and steric hindrance on promoting methyl lactate dehydration beyond the strength and structure of pyridine.[25] High basicity favors stronger BAS titration, while steric constraints limit binding on BAS due to internal diffusion limitations and local steric interactions. Titrants with a basicity above 972 kJ/mol and a van der Waals diameter below 6.2 Å were predicted to afford a dehydration selectivity above 90%. Based on the predicted criteria, 1,1,3,3-tetramethylguanidine (TMG) was demonstrated by experiment to improve dehydration selectivity to 89% from the baseline performance of 61% over Na-FAU. However, conversion was unstable after five hours of time on stream, potentially due to the low stability of TMG at 300 ºC.[25]

Notably, most of the molecules that were predicted to improve selectivity above 90% have
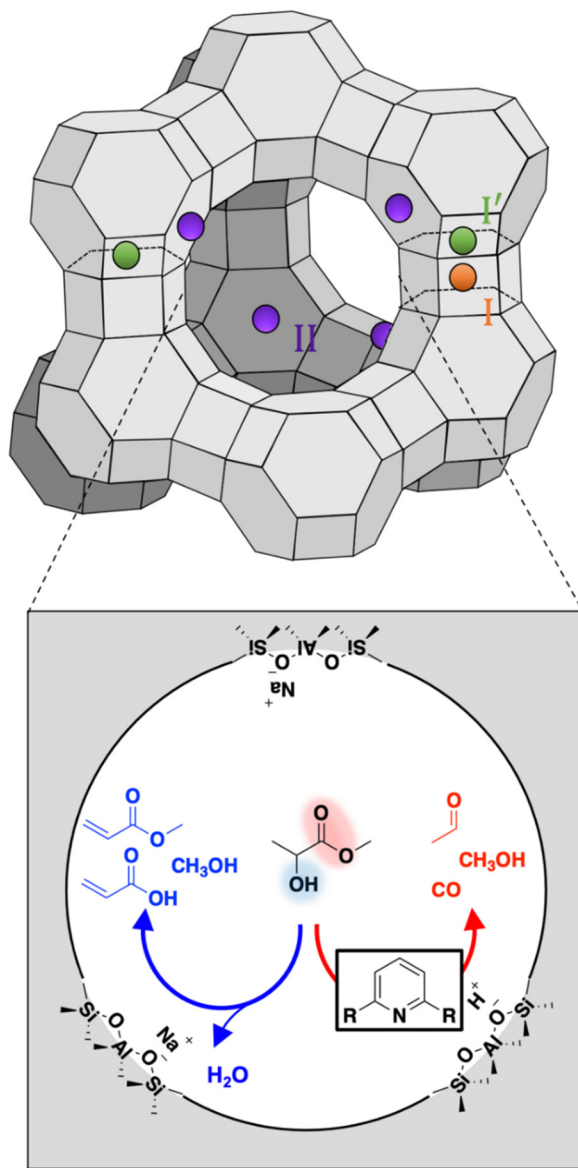
Figure 1. A representative distribution of sodium cations on site I, I', and II for Na-FAU (Si/Al = 2.6) is shown on a faujasite structure obtained from Hattori et al.[58] On average, each supercage structure may have four cations on site II, two on site I', and one on site I which are shown in purple, green, and orange, respectively at representative locations within the FAU structure. Two major pathways for methyl lactate on Na-FAU are shown on the right: (i) dehydration (blue) to acrylic acid and methyl acrylate on sodium acid site; (ii) decarbonylation (red) to acetaldehyde, methanol, and carbon monoxide. Introduction of a basic titrant can suppress decarbonylation.

more than one amine or basic functional groups, prompting the consideration of simultaneous
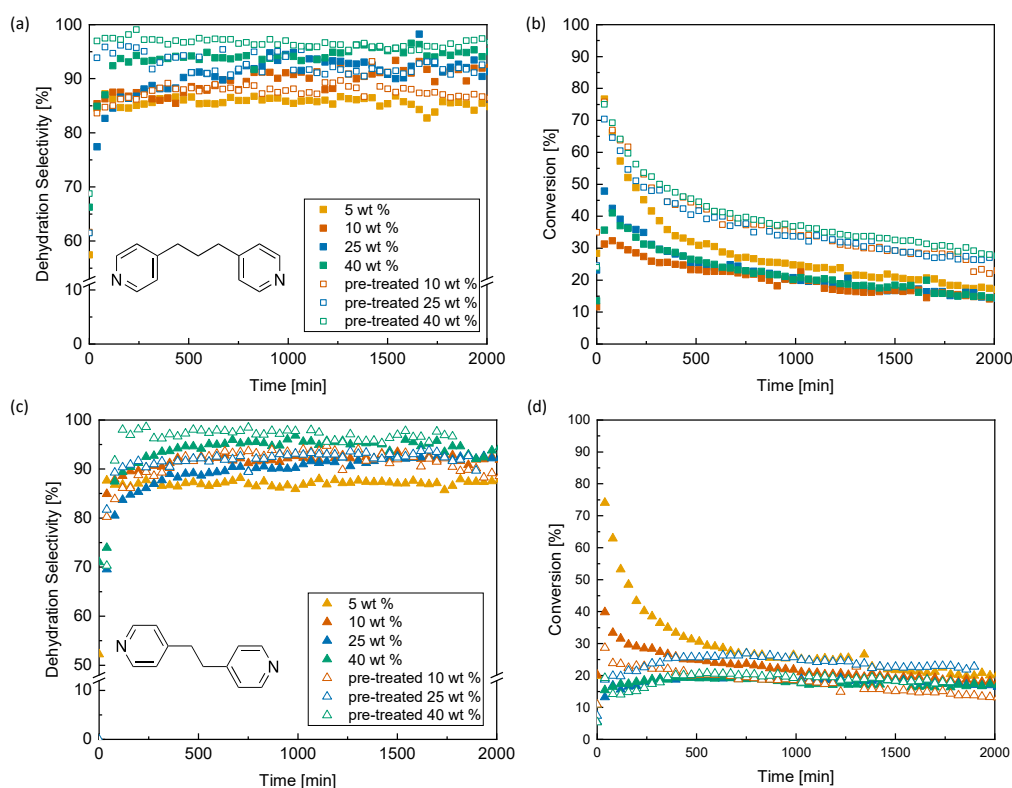
Figure 2. Time-on-stream dehydration reactivities of methyl lactate to acrylic acid and methyl acrylate were evaluated with the addition of 4,4′-trimethylenedipyridine (44TMDP) and 1,2-bis(4-pyridyl)ethane (1,2BPE). Data with 44TMDP are shown in squares in **(a)** and **(b)**. Data with 12BPE are shown in triangles in **(c)** and **(d)**. The amines were loaded using wet impregnation at varying loadings. The solid symbols represent experiments using the amine loaded Na-FAU catalyst as prepared. The open symbols represent experiments using the amine loaded Na-FAU catalyst after pre-treating the catalyst at 300 ℃ under helium flow at 90 mL min⁻¹ for 500 min. Reaction condition: 300 ℃, P_{tot} = 101.3 kPa ($P_{methyllactate}$ = 78.0 Pa, P_{water} = 1.1 kPa, balanced by helium at a flowrate of 90 mL min⁻¹), and WHSV = 0.9 h⁻¹.

adsorption on multiple BAS with one multifunctional amine molecule. The structure of Na-FAU consists of small, six-membered ring (6-MR) sodalite cages (*sod*, diameter of 6.3 Å) connected by double six rings (*d6r*) to form large accessible supercages (diameter of 11.2 Å) having 12-MR openings of 7.4 Å (**Figure 1**).[29,30] The Na-FAU catalyst used in our previous work[25] and this work has a Si/Al ratio of 2.6. This high aluminum content correlates to a high density of acid sites in the materials. On average, seven sodium cation sites are present per supercage. At room temperature, four sodium cations may be located, on average, at the readily accessible site II, while three may be embedded in the less accessible locations in the sodalite cages with two at site I' and one at site I.[31–36] However, molecular adsorption can change the position of the sodium cations on

site I and I' to the more accessible site II positions in the supercage.[31,37] Potentially, adsorbates may interact with all seven sodium cation sites and generate *in situ* BAS. Titrants with multiple basic functional groups may provide a higher overall site coverage compared with the titrants with a single basic group.

Results and Discussion. In this work, two multifunctional flexible amines were added within the pores of the zeolite catalyst for enhancing selectivity to acrylic acid and methyl acrylate via dehydration of methyl lactate. The multifunctional amines were loaded onto Na-FAU via wet impregnation at nominal loadings of 5, 10, 25, and 40 wt% of the Na-FAU framework for independent trials using the method described in Supporting Information Section S1. In summary, the amine and

Na-FAU were stirred in methanol at room temperature for four hours before being dried at 70 °C for 24 hours. Notably, wet impregnation was not performed in an environment free of moisture. The final amine loadings deviate slightly from the nominal loading, due to the presence of water in the Na-FAU materials, as determined by thermogravimetric analysis.

The impregnated catalysts were then evaluated for methyl lactate dehydration (details in Supporting Information Section S2). Dehydration selectivity of 96±3% was achieved for 2000 min time on stream with 4,4′-trimethylenedipyridine (44TMDP, **Figure 2a** and **b**) and 1,2-bis(4-pyridyl)ethane (12BPE, **Figure 2c** and **d**) at 300 °C. The selectivity is the highest for lactate dehydration reported to date and has exceeded the desirable value of 90% for commercial viability. Notably, induction periods were observed; dehydration selectivity initially started at lower values and gradually achieved higher steady values after approximately 500 min time on stream (**Figure 2a** and **c**). Steady state dehydration selectivity increased from 85 to 96% with the increase in amine loading from 5 to 40 wt%. Initial conversion decreased from ~80% to 45% with 44TMDP and to 15% with 12BPE with the increase in amine loading from 5 to 40 wt% (**Figure 2b** and **d**). However, after 500 min time on stream, conversion became similar across varying amine loadings of both 44TMDP or 12BPE.

The induction periods are proposed to result from poor distribution of multifunctional amines throughout FAU particles during wet impregnation due to slow diffusion. In our previous study,[25] larger amine size correlated with slower diffusion in FAU pores. 2,6-diisopropylpyridine (6.6 Å) and 2,6-ditertbutylpyridine (7.0 Å) were calculated to diffuse one and two orders of magnitude slower than methyl lactate in zeolite FAU.[25] In this work, the calculated van der Waals (vdW) diameter (Supporting Information Section S3) of 12BPE and 44TMDP are 6.6 and 6.8 Å, which are 89 and 91%, respectively, of the 12-MR window between supercages in FAU zeolite. When initially impregnated in FAU particles, amines likely reside within the pores near the particle exterior; this prevents BAS titration by 12BPE and 44TMDP and causes pore blockages. However, provided sufficient time, the multifunctional amines access

more supercages and internal BAS, affording more effective BAS titration and catalytic control.

To evaluate the induction periods, catalyst preparation methods were modified to improve amine distribution prior to reaction. The FAU catalysts impregnated with amines were pretreated in helium flow at 90 mL min⁻¹ for 500 min prior to catalyzing methyl lactate dehydration. As shown in **Figure 2**, thermal pre-treatment shortened the induction periods to about 80 to 120 min for samples with amine loadings of 25 and 40 wt%. Additionally, after pre-treatment, a steady selectivity above 96% was still achieved with Na-FAU loaded with either 44TMDP or 12BPE at an initial nominal loading of 40 wt%. For the pretreated Na-FAU impregnated with 44TMDP, conversion of methyl lactate was similar for multiple amine loadings of 10, 25, and 40 wt% (**Figure 2b**). Compared with the samples without pre-treatment, an improvement in initial conversion was also observed from ~45% to 75% after pre-treatment. For the Na-FAU catalysts loaded with 12BPE, no significant change in long-time conversion was observed before and after pre-treatment (**Figure 2d**).

Catalyst stability with time on stream differed between Na-FAU loaded with 44TMDP and 12BPE. Na-FAU zeolite impregnated with 44TMDP at loadings of 25 and 40 wt% exhibited decreasing conversion by half of the initial values after 1000 min time on stream with or without pre-treatment. However, Na-FAU impregnated with 12BPE at the same loadings showed steady conversion at 25 and 20%, respectively, over 2000 min. Catalyst deactivation has been proposed to occur via coking from the decarbonylation pathway and pore blocking by bulky compounds formed by amine and acrylic acid.[28] At a much lower conversion of 20% and dehydration selectivity around 96% with 12BPE, coking from decarbonylation and pore blockage from bulky compounds are believed to be small contributions to catalyst deactivation, which could explain the higher catalyst stability with the 12BPE impregnated Na-FAU.

Amine loading following pre-treatment and reaction was quantified using thermogravimetric analysis (TGA) coupled with mass spectrometry (MS) as shown in **Figure 3**. Prior to the TGA experiment, the impregnated catalyst samples were first heated to 300 ºC in helium for 3000 min and
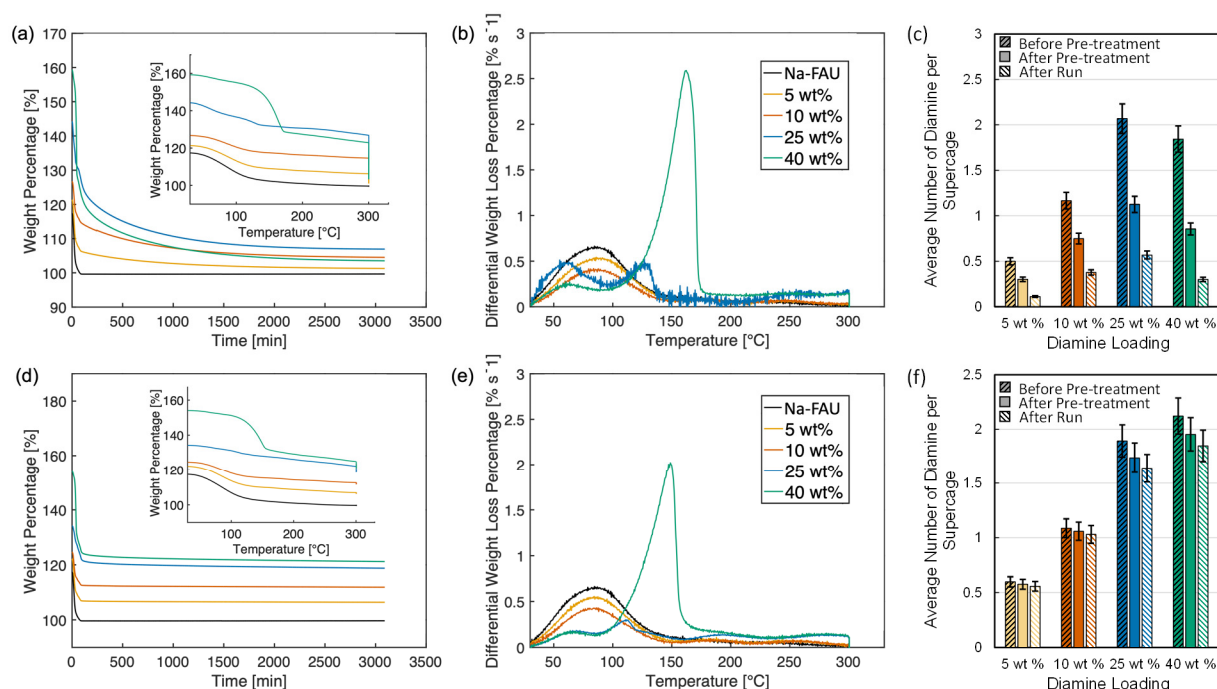
Figure 3. Thermo-gravimetric analysis of Na-FAU impregnated with **(a)** – **(c)** 4,4′-trimethylenedipyridine (44TMDP) and **(d)** – **(e)** 1,2-bis(4-pyridyl)ethane (12BPE) at variable loadings are presented as weight percentage over time and temperature, differential weight percentage over temperature, and average number of diamine per supercage before and after pre-treatment, and after run. The mass of Na-FAU framework in each sample is denoted as a weight percentage of 100%. Error bars in (c) and (f) denote 95% confidence intervals estimated from repeated experiments.

then to 550 ºC in air to remove any organic residues; the mass of the Na-FAU framework at the end of the trial was denoted as 100 wt%. A detailed TGA-MS procedure is provided in Supporting Information Section S4.

Rapid decreases in weight percentage were observed in TGA-MS experiments with all catalyst samples in the first 90 min, which was the time required to reach 300 ºC (**Figure 3a** and **d**). As temperature linearly increased from 30 to 300 ºC at a ramp rate of 3 ºC min^{-1}, the differential weight loss percentage, calculated as the negative rate in weight loss, exhibited several peaks, indicating rapid loss of chemical species during specific temperature regimes (**Figure 3b** and **3e**). Evolving chemical species from the catalyst were identified with a mass spectrometer, which showed that 44TMDP only started leaving Na-FAU at 300 ºC (**Figure S2c** and **S2d**), while 12BPE would leave Na-FAU earlier at 210 ºC (**Figure S2a** and **S2b**). No methanol was detected in any sample (**Figure S1a** and **S1b**, Supporting Information Section S4).

Most of the water was removed as the temperature increased from 50 to 300 ºC (**Figure**

S2). Therefore, the major peaks in **Figure 3b** and **3e** under 200 °C are assigned as water. The actual loadings of amines on Na-FAU can therefore be estimated by the weight percentage at 300 ºC for 44TMDP and 210 ºC for 12BPE (**Table S1**). Notably, the loading of 5, 10, and 25 wt% from wet impregnation resulted in similar actual loadings. However, amine uptake appeared to plateau after 25 wt% loading from wet impregnation. The 40 wt% loading from wet impregnation only afforded an actual loading of 23 and 25 wt% for 44TMDP and 12BPE, respectively. Once the temperature reached 300 ºC, 44TMDP loading continued to decrease with time, while 12BPE loading stayed relatively constant over 3000 min. As temperature reached 300 ºC after 90 min, the weight percentages at 90, 590, and 2590 min time on stream in TGA can be used to estimate the loadings of amine per supercage before pre-treatment, after 500 min pre-treatment, and after reaction run of 2000 min time on stream, respectively.

The average number of diamines per supercage was calculated by dividing the moles of amine in the zeolite by the moles of supercages in FAU
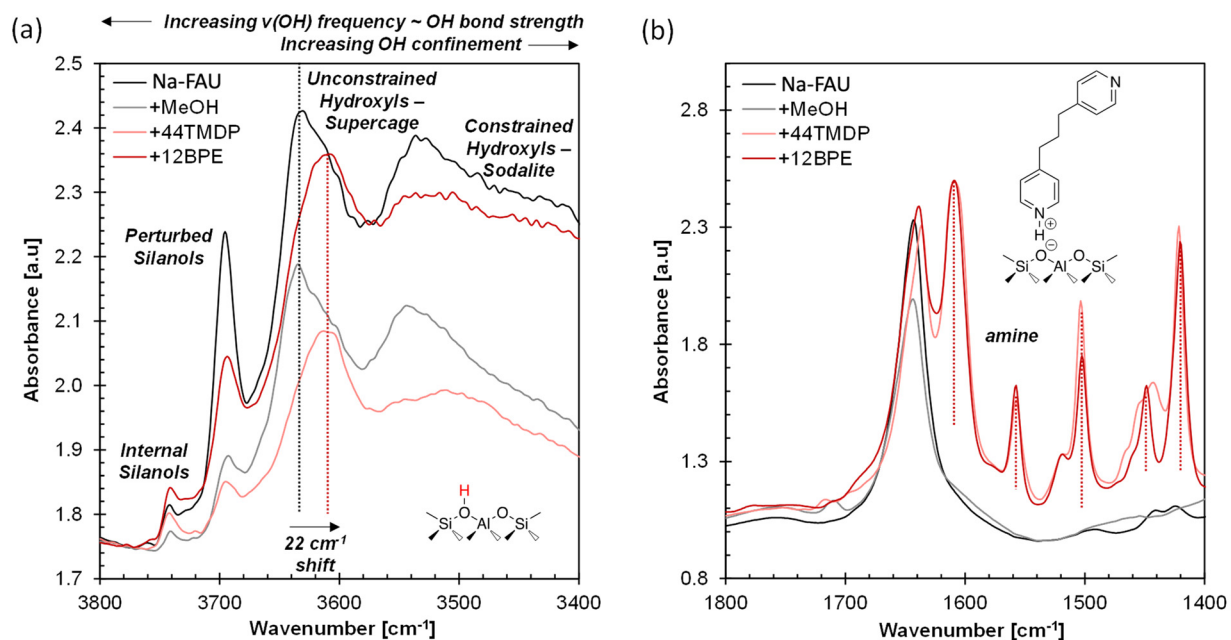
Figure 4. Fourier-transformed Infrared Spectroscopy scans were used to elucidate interactions between multifunctional amines and internal active sites of Na-FAU (in black), Na-FAU stirred in methanol (in grey), Na-FAU impregnated with 44TMDP at a loading of 40 wt% (in orange), and Na-FAU impregnated with 12BPE at a loading of 40 wt%(in red) over the wavenumber of 1000 to 4000 cm^{-1}.

zeolite (details in Supporting Information Section S4).[38–40] Before pre-treatment, approximately 0.5, 1.2, 2.1, and 1.8 molecules of 44TMDP were loaded per supercage for the nominal loadings of 5, 10, 25, 40 wt% from wet impregnation (**Figure 3c**). The difference in number of 44TMDP per supercage for nominal loadings of 25 and 40 wt% is within experimental error. After pre-treatment, the loading decreased by 36 – 52% to approximately 0.30, 0.75, 1.1, and 0.85 molecule per supercage of Na-FAU. Each supercage contains, at our highest loading, an average of two 44TMDP prior to pre-treatment and one after pre-treatment; about one molecule per supercage evaporates and leaves the particle during pre-treatment. At 2590 min (2000 min after pre-treatment at 300 ºC), the loading of 44TMDP further decreased by 26 – 38% to 0.1, 0.4, 0.6, and 0.3 molecule per supercage. In total, approximately 68 – 83% of 44TMDP was removed during the reaction times studied here compared with the loading before pre-treatment. At a maximum loading of one molecule per supercage, 44TMDP only occupies about 24% of the supercage occupiable volume (details in Supporting Information Section S4), leaving more active sites

accessible to methyl lactate. Moreover, as more than half of the 44TMDP gradually leaves the supercages during reaction, the amines may interact with acrylic acid, methanol, or other products to form bulkier molecules that can result in pore blockages. Therefore, the initial conversion with 44TMDP was as high as 75% but decreased to 30% after 2000 min time on stream at amine nominal loadings of 10, 25, and 40 wt% with pre-treatment (**Figure 2b**).

In contrast, 12BPE predominately remained within the FAU zeolite particles, even after pretreatment and reaction. Before pre-treatment, each supercage hosted approximately 0.6, 1.1, 1.9, and 2.1 12BPE molecules with the increase in 12BPE nominal loadings from 5 to 40 wt% (**Figure 3f**). The volume of two 12BPE molecules accounts for ~45% of the occupiable volume of the supercage (details in Supporting Information Section S4). After pre-treatment, 12BPE loading only decreased by 3 – 8% for different loadings, which is consistent with the insignificant change in conversion observed with 12BPE after pre-treatment in **Figure 2b** and **2d**. Even after 2000 min at 300 ºC, the loading of 12BPE exhibited no significant change. The steady loading of 12BPE is

consistent with the stable conversion of methyl lactate over long time on stream (**Figure 2d**). Due to the proclivity of 12BPE to remain in Na-FAU catalysts, reactions exhibited steady and almost complete suppression of the deactivating decarbonylation side reaction as indicated by the consistent dehydration selectivity of 96±3%.

The interaction between the multifunctional amines and the internal active sites of Na-FAU (**Figure 4**) was assessed via Fourier-transform infrared (FTIR) spectroscopy. FTIR spectra were collected after Na-FAU materials were impregnated with diamine, pretreated, and then heated to 200 ºC to remove the majority of water and cooled down to 25 ºC within the FTIR sample cell. Experimental methods are detailed in Supporting Information Section S5. Two signature peaks for bridging hydroxyl groups in FAU were observed as expected: in the supercage at 3650 cm^{-1} and in the sodalite cages at 3540 cm^{-1}.[41–43] Background scans of Na-FAU prior to diamine addition showed bands at 3740 cm^{-1} and 3690 cm^{-1}, which are attributed to isolated internal silanol groups and hydrogen-bonded silanol groups[44], respectively.[45] Unconstrained hydroxyl groups, indicating the presence of Brønsted acid sites (BAS) in the supercages of Na-FAU, are indicated by the band at 3633 cm^{-1}.[41,45,46] The shift from 3650 to 3633 cm^{-1} could be due to weak interactions between the hydroxyl groups and water molecules.[47] Constrained hydroxyl groups, indicating the BAS in the sodalite cages, are assigned to the band at 3540 cm^{-1}.[41,45,46] The presence of BAS in Na-FAU is surprising since no methanol dehydration activity was observed in Na-FAU at 300 ºC in our previous work,[25] though a minimal amount of Brønsted acidity (< 29 $\mu mol\ (g_{cat})^{-1}$) was measured on the Na-FAU materials.[25]

FTIR spectra revealed distinct differences in hydroxyl interactions upon impregnation of amine (**Figure 4**). When amines were inside Na-FAU pores, the band associated with unconstrained (supercage) hydroxyls shifted by 22 cm^{-1} from 3633 cm^{-1} to 3611 cm^{-1}, indicating elongated O-H bond of the hydroxyls and weakened hydrogen bonding interactions.[48] This effect is believed to be caused by the interactions between 12BPE or 44TMDP with the internal BAS in supercages. The bands at 1600, 1555, and 1500 cm^{-1} can be partially attributed to hydrogen-bonded pyridine functional groups[49] and the N-H vibrations of the amine molecules.[50,51] To isolate the effect of methanol on the formation of BAS during the wet impregnation process, Na-FAU was stirred in methanol for four hours and dried using the same method detailed in Supporting Information Section S1. No shift of the hydroxyl bands at 3633 and 3540 cm^{-1} was observed in the methanol treated Na-FAU compared with Na-FAU, confirming that the 22 cm^{-1} shift is most likely due to the presence of amines interacting with hydroxyls in the supercage, and not simply methanol.

Our experiments using multifunctional amines in Na-FAU to suppress side reactions have demonstrated the highest observed dehydration selectivity from methyl lactate to acrylates. Dehydration selectivity to acrylic acid and acrylate of 96±3% was achieved at an initial conversion of 75% with 44TMDP and 18% with 12BPE at a loading of 40 wt% with pre-treatment at 0.9WHSV (**Figure 2**). Therefore, we expanded our investigation of multifunctional amines to two additional dipyridines with alternate chain lengths and flexibility, in an initial search for additional basic titrants desirable for methyl lactate dehydration (**Figure 5a**). After pre-treatment at a loading of 40 wt%, 12BPE and 44TMDP still showed the highest selectivity among the selected amines at the same weighted hourly space velocity (WHSV, defined as Equation S1 of the Supporting Information) of 0.9 h^{-1} albeit across a range of conversions. Similar initial conversion of 20-30% was achieved with each amine modifier by tuning WHSV from 0.9 to 8.4 h^{-1}. At similar conversion, 12BPE and 44TMDP still showed the highest selectivity of 96% and 91%, respectively, among the four amines (**Figure 5a**). Interestingly, dehydration selectivity was only weakly dependent on conversion over a range of conversion from 20 to 96% over Na-FAU and 44TMDP loaded Na-FAU (data guided by the dashed lines in **Figure 5b**). Notably, the selectivity with 4,4′-dipyridyl (44DP, *c* in **Figure 5**) and 1,2-di(4-pyridyl)ethylene (12D4P, *d* in **Figure 5**) was 10% lower than the 96% selectivity achieved with 12BPE. We attribute the lower selectivity to a lower degree of flexibility in the tethering between two pyridine functional groups in 44DP and 12D4P, limiting the effectiveness of titrating multiple BAS by these amines.
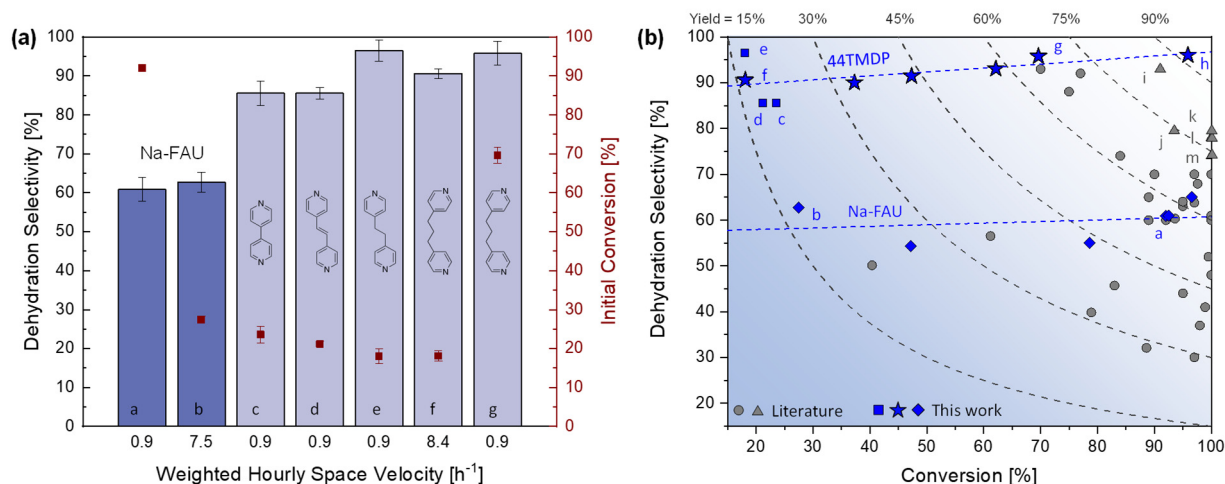
Figure 5. (a) Methyl lactate dehydration selectivity was evaluated over Na-FAU catalyst impregnated with multifunctional amines at the loading of 40 wt% with pre-treatment. Bar a and b were obtained over Na-FAU without amines at a weighted hourly space velocity (WHSV) of 0.9 and 7.5 h^{-1}, respectively. Bar c, d, and e were over Na-FAU impregnated with 4,4′-dipyridyl, 1,2-di(4-pyridyl)ethylene, and 12BPE at a WHSV of 0.9 h^{-1}. Bar f and g were over Na-FAU impregnated with 44TMDP at a WHSV of 8.4 and 0.9 h^{-1}, respectively. Reaction condition: 300 ℃, P_{tot} = 101.3 kPa ($P_{methyllactate}$ = 78.0 Pa, P_{water} = 1.1 kPa, balanced by helium at a flowrate of 90 mL min^{-1}). Detailed information about the amines is listed in **Table S2. (b)** Methyl lactate dehydration activities over amine impregnated Na-FAU in this work are compared with values from literature over zeolites, inorganic salts, and hydroxyapatite catalysts.[5,6,18–22,57,59–61,7,8,10–12,14,15,17] Datapoint *a – g* are the same data from **(a)**. Datapoint *i – m* are example data from the literature (**Table S3**).[5,6,8,14,22,57] A minimal dependence of selectivity on conversion was observed across varying WHSV of 0.6 – 7.5 h^{-1} over Na-FAU (in blue diamonds) and 0.2 – 8.4 h^{-1} over 44TMDP impregnated Na-FAU at 40 wt% nominal loading (in blue stars). Dashed lines were included to guide the eyes.

Among the selected amines in **Figure 5a**, 44TMDP (data point g in **Figure 5**) afforded a yield as high as 70% to acrylic acid and methyl lactate. Reducing the WHSV from 0.9 to 0.2 h^{-1} pushed initial conversion to 96% at a selectivity of 96% with 44TMDP, giving the highest yield of 92% reported for methyl lactate or lactic acid dehydration (data point h in **Figure 5b**). Notably, the highest selectivity previously achieved over zeolites was typically in the range of 50-70% at almost complete conversion.[17,19,21] To achieve this previously reported selectivity, zeolites were typically modified with potassium or other metal cations. Recently, a study using potassium-modified ZSM-5 zeolite afforded a selectivity of 80% at a conversion of 100% (data point k in **Figure 5b**).[22] Additional high-performing catalysts from the literature are typically inorganic salts.[8,9,14,16] The highest yield in the literature is 85% at a selectivity of 93% over phosphate salts at 350 ℃ reported in a US patent from Lingoes and Collias (data point i in **Figure 5b**).[8] Other desirable catalysts were also mostly phosphate or sulfate salts

(data point *j*[16] and *m*[9] in **Figure 5b**) or hydroxyapatite (data point *l*[14] in **Figure 5b**), affording yields around 70-80%. However, in general these salts require higher reaction temperature in the range of 340 – 400 ℃. Our system, demonstrating the highest yield of 92% to date while operating at a lower temperature of 300 ℃ using commercial zeolite materials with mild modification, further promotes the use of biomass-derived methyl lactate as an alternative feedstock to acrylates. Future work will focus on catalyst stability and the interactions between multifunctional amines and acid sites in the supercages of Na-FAU.

2.0 Conclusions. In conclusion, we reported the highest dehydration selectivity of 96% and yield of 92% from methyl lactate to acrylates over Na-FAU impregnated with multifunctional amines, including 44TMDP and 12BPE. Steady state dehydration selectivity increased from 85 to 96% as the nominal loadings of 44TMDP or 12BPE increased from 5 to 40%. However, an induction

period of approximately 500 min was observed. Pre-treating the impregnated Na-FAU under helium flow at 300 ºC significantly reduced the induction periods while maintaining the high dehydration selectivity of 96%. Conversion was improved from 40-50% to 75% with pre-treatment for the 44TMDP impregnated Na-FAU, but no significant change was observed for the 12BPE loaded Na-FAU. 44TMDP loaded Na-FAU samples also showed faster deactivation compared with the 12BPE loaded samples. TGA-MS determined that loading of 44TMDP decreased by 36 – 52% after pre-treatment and continued to drop until only 17 – 32% remained after 2000 min at the reaction temperature of 300 ºC. However, the loading of 12BPE after pre-treatment and 2000 min at reaction temperature remained effectively unchanged. The results are consistent with the increase in conversion with pre-treatment observed over the 44TMDP impregnated Na-FAU but not on the 12BPE impregnated Na-FAU. FTIR indicated interactions between diamines with BAS within supercages of Na-FAU, demonstrating that 44TMDP and 12BPE enters Na-FAU window openings. Further investigation with varying connectivity between amines and reaction optimization afforded the highest yield to acrylates of 92% at a selectivity of 96% over 44TMDP impregnated Na-FAU. This is the highest performance reported to date, exceeding the target selectivity and yield of 90% for commercial viability. The use of multifunctional amines can be extended to reaction systems where BAS are responsible for side reactions. Mechanistic insights comparing the adsorption of single amines and classes of multifunctional amines are under further investigation.

Keywords. Lactic Acid, Acrylic Acid, Zeolite, Amine, Dehydration

Supporting Information. The Supporting information is available free of charge online (http://xyz) and addresses the following:

Materials Preparation; Reaction Activity Measurements; Molecular Size Descriptors; Thermogravimetric Analysis (TGA) – Mass Spectrometry (MS); Fourier-Transformed Infrared (FTIR) Spectroscopy; Additional Multifunctional Amines and Comparison with Literature Values. The supporting information references additional publications.[14,52–57]

References
(1) Dusselier, M.; Van Wouwe, P.; Dewaele, A.; Makshina, E.; Sels, B. F. Lactic Acid as a Platform Chemical in the Biobased Economy: The Role of Chemocatalysis. *Energy Environ. Sci.* **2013**, *6*, 1415–1442.
(2) Matt Blois. Companies Tiptoe Back to Biobased Acrylic Acid. *Chemical & Engineering News*. 2021.
(3) Sprenger, P.; Kleist, W.; Grunwaldt, J. D. Recent Advances in Selective Propylene Oxidation over Bismuth Molybdate Based Catalysts: Synthetic, Spectroscopic, and Theoretical Approaches. *ACS Catal.* **2017**, *7*, 5628–5642.
(4) NEXANT. *Acrylic Acid and Esters NEXANT PERP Reports 2013-2019*; 2019.
(5) Lira, C. T.; McCrackin, P. J. Conversion of Lactic Acid to Acrylic Acid in Near-Critical Water. *Ind. Eng. Chem. Res.* **1993**, *32*, 2608–2613.
(6) Paparizos, C.; Dolhyi, S. R.; Shaw, W. G. US4786756A, 1988.
(7) Robert A. Sawicki. US4729978, 1988.
(8) Lingoes, J. V.; Collias, D. I. US9926256B2, 2018.
(9) Peng, J.; Li, X.; Tang, C.; Bai, W. Barium Sulphate Catalyzed Dehydration of Lactic Acid to Acrylic Acid. *Green Chem.* **2014**, *16*, 108–111.
(10) Zhang, Z.; Qu, Y.; Wang, S.; Wang, J. Catalytic Performance and Characterization of Silica Supported Sodium Phosphates for the Dehydration of Methyl Lactate to Methyl Acrylate and Acrylic Acid. *Ind. Eng. Chem. Res.* **2009**, *48*, 9083–9089.
(11) Wang, B.; Li, C.; Zhu, Q.; Tan, T. The Effect of K2HPO4 and Al2(SO4)3modified MCM-41 on the Dehydration of Methyl Lactate to Acrylic Acid. *RSC Adv.* **2014**, *4*, 45679–45686.

(12) Dongare, M. K.; Umbarker, S. B.; Lomate, S. T. US8957250B2, 2006.

(13) Yan, B.; Tao, L.; Liang, Y.; Xu, B. Sustainable Production of Acrylic Acid : Catalytic Performance of Hydroxyapatites for Gas-Phase Dehydration of Lactic Acid. *ACS Catal.* **2014**, *4*, 1931–1943.

(14) Ghantani, V. C.; Dongare, M. K.; Umbarkar, S. B. Nonstoichiometric Calcium Pyrophosphate : A Highly e Fficient and Selective Catalyst for Dehydration of Lactic Acid to Acrylic Acid. *RSC Adv.* **2014**, *4*, 33319–33326.

(15) Näfe, G.; Traa, Y.; Hirth, T.; Klemm, E. True Catalytic Behavior of Lactic Acid Dehydration on Zeolite Na-Y in the Gas Phase Measured by Means of a Novel Apparatus Design. *Catal. Letters* **2014**, *144*, 1144–1150.

(16) Zhang, J.; Zhao, Y.; Feng, X.; Pan, M.; Zhao, J.; Ji, W.; Au, C. T. Na2HPO4-Modified NaY Nanocrystallites: Efficient Catalyst for Acrylic Acid Production through Lactic Acid Dehydration. *Catal. Sci. Technol.* **2014**, *4*, 1376–1385.

(17) Yan, B.; Tao, L. Z.; Liang, Y.; Xu, B. Q. Sustainable Production of Acrylic Acid: Alkali-Ion Exchanged Beta Zeolite for Gas-Phase Dehydration of Lactic Acid. *ChemSusChem* **2014**, *7*, 1568–1578.

(18) Shi, H. F.; Hu, Y. C.; Wang, Y.; Huang, H. KNaY-Zeolite Catalyzed Dehydration of Methyl Lactate. *Chinese Chem. Lett.* **2007**, *18*, 476–478.

(19) Yan, B.; Mahmood, A.; Liang, Y.; Xu, B. Q. Sustainable Production of Acrylic Acid: Rb+- and Cs+-Exchanged Beta Zeolite Catalysts for Catalytic Gas-Phase Dehydration of Lactic Acid. *Catal. Today* **2016**, *269*, 65–73.

(20) Sun, P.; Yu, D.; Fu, K.; Gu, M.; Wang, Y.; Huang, H.; Ying, H. Potassium Modified NaY: A Selective and Durable Catalyst for Dehydration of Lactic Acid to Acrylic Acid. *Catal. Commun.* **2009**, *10*, 1345–1349.

(21) Sun, P.; Yu, D.; Tang, Z.; Li, H.; Huang, H. NaY Zeolites Catalyze Dehydration of Lactic Acid to Acrylic Acid: Studies on the Effects of Anions in Potassium Salts. *Ind. Eng. Chem. Res.* **2010**, *49*, 9082–9087.

(22) Makshina, E. V; Canadell, J.; Krieken, J. Van; Sels, B. F. Potassium-Modified ZSM-5 Catalysts for Methyl Acrylate Formation from Methyl Lactate: The Impact of the Intrinsic Properties on Their Stability and Selectivity. **2022**, *10*, 6196–6204.

(23) Noda, Y.; Zhang, H.; Dasari, R.; Singh, R.; Ozmeral, C.; Román-Leshkov, Y.; Rioux, R. M. Importance of Dimer Quantification for Accurate Catalytic Evaluation of Lactic Acid Dehydration to Acrylic Acid. *Ind. Eng. Chem. Res.* **2017**, *56*, 5843–5851.

(24) Losada, M.; Tran, H.; Xu, Y. Lactic Acid in Solution: Investigations of Lactic Acid Self-Aggregation and Hydrogen Bonding Interactions with Water and Methanol Using Vibrational Absorption and Vibrational Circular Dichroism Spectroscopies. *J. Chem. Phys.* **2008**, *128*, 1–11.

(25) Pang, Y.; Ardagh, M. A.; Shetty, M.; Chatzidimitriou, A.; Kumar, G.; Vlaisavljevich, B.; Dauenhauer, P. J. On the Spatial Design of Co-Fed Amines for Selective Dehydration of Methyl Lactate to Acrylates. **2021**, *11*, 5718–5735.

(26) Murphy, B. M.; Letterio, M. P.; Xu, B. Selectivity Control in the Catalytic Dehydration of Methyl Lactate: The Effect of Pyridine. *ACS Catal.* **2016**, *6*, 5117–5131.

(27) Murphy, B. M.; Letterio, M. P.; Xu, B. Catalytic Dehydration of Methyl Lactate: Reaction Mechanism and Selectivity Control. *J. Catal.* **2016**, *339*, 21–30.

(28) Murphy, B. M.; Letterio, M. P.; Xu, B. Catalyst Deactivation in Pyridine-Assisted Selective Dehydration of Methyl Lactate on NaY. *ACS Catal.* **2017**, *7*, 1912–1930.

(29) Baerlocher, C.; McCusker, L. B. Database of Zeolite Structures. *Available at: http://www.iza-structure.org/databases/* **2014**, Accessed online: January 2014. https://doi.org/http://www.iza-structure.org/databases/.

(30) Rouquerol, F.; Rouquerol, J.; Sing, K. Adsorption by Clays, Pillared Layer Structures and Zeolites. *Adsorpt. by Powders Porous Solids* **1999**, 355–399.

(31) Ramsahye, N. A.; Bell, R. G. Cation Mobility and the Sorption of Chloroform in Zeolite NaY: Molecular Dynamics Study. *J. Phys. Chem. B* **2005**, *109*, 4738–4747.

(32) Buttefey, S.; Boutin, A.; Fuchs, A. H. Cation Distribution in Faujasite-Type Zeolites: A Test of Semi-Empirical Force Fields for Na Cations. *Mol. Simul.* **2002**, *28*, 1049–1062.

(33) Van Dun, J. J.; Mortier, W. J. Temperature-Dependent Cation Distribution in Zeolites. 1. A Statistical Thermodynamical Model. *J. Phys. Chem.* **1988**, *92*, 6740–6746.

(34) Beauvais, C.; Boutin, A.; Fuchs, A. H. A Numerical Evidence for Nonframework Cation Redistribution upon Water Adsorption in Faujasite Zeolite. *ChemPhysChem* **2004**, *5*, 1791–1793.

(35) Beauvais, C.; Guerrault, X.; Coudert, F. X.;

Boutin, A.; Fuchs, A. H. Distribution of Sodium Cations in Faujasite-Type Zeolite: A Canonical Parallel Tempering Simulation Study. *J. Phys. Chem. B* **2004**, *108*, 399–404.

(36) Louisfrema, W.; Rotenberg, B.; Porcher, F.; Paillaud, J. L.; Massiani, P.; Boutin, A. Cation Redistribution upon Dehydration of Na58Y Faujasite Zeolite: A Joint Neutron Diffraction and Molecular Simulation Study. *Mol. Simul.* **2015**, *41*, 1371–1378.

(37) Jaramillo, E.; Grey, C. P.; Auerbach, S. M. Molecular Dynamics Studies of Hydrofluorocarbons in Faujasite-Type Zeolites: Modeling Guest-Induced Cation Migration in Dry Zeolites. *J. Phys. Chem. B* **2001**, *105*, 12319–12329.

(38) Jelinek, R.; Özkar, S.; Pastore, H. O.; Malek, A.; Ozin, G. A. Guest-Host Interactions in Sodium Zeolite Y: Structural and Dynamical 23Na Double-Rotation NMR Study of H2O, PMe3, Mo(CO)6, and Mo(CO)4(PMe3)2 Adsorption in Na56Y. *J. Am. Chem. Soc.* **1993**, *115*, 563–568.

(39) Moon, D. J.; Lim, W. T. Synthesis and Single-Crystal Structure of Sodium Sulfide Cationic Cluster in the Sodalite Cavity of Zeolite Y (FAU, Si/Al = 1.56). *J. Porous Mater.* **2020**, *27*, 1233–1240.

(40) Su, H.; Kim, H. S.; Seo, S. M.; Ko, S. O.; Suh, J. M.; Kim, G. H.; Lim, W. T. Location of Na + Ions in Fully Dehydrated Na +- Saturated Zeolite y (FAU, Si/Al = 1.56). *Bull. Korean Chem. Soc.* **2012**, *33*, 2785–2788.

(41) Lakiss, L.; Kouvatas, C.; Gilson, J. P.; Aleksandrov, H. A.; Vayssilov, G. N.; Nesterenko, N.; Mintova, S.; Valtchev, V. Unlocking the Potential of Hidden Sites in Faujasite: New Insights in a Proton Transfer Mechanism. *Angew. Chemie - Int. Ed.* **2021**, *60*, 26702–26709.

(42) Jacobs, P. A.; Mortier, W. J. An Attempt to Rationalize Stretching Frequencies of Lattice Hydroxyl Groups in Hydrogen-Zeolites. *Zeolites* **1982**, *2*, 226–230.

(43) Wakabayashi, F.; Kondo, J. N.; Domen, K.; Hirose, C. FT-IR Study of the Interaction of Oxygen, Argon, Helium, Nitrogen and Xenon with Hydroxyl Groups in H-Y Zeolite at Low Temperatures. *Microporous Mater.* **1997**, *8*, 29–37.

(44) Dalstein, L.; Potapova, E.; Tyrode, E. The Elusive Silica/Water Interface: Isolated Silanols under Water as Revealed by Vibrational Sum Frequency Spectroscopy. *Phys. Chem. Chem. Phys.* **2017**, *19*, 10343–10349.

(45) Bordiga, S.; Lamberti, C.; Bonino, F.; Travert, A.; Frédéric, T.-S.; Thibault-Starzyk, F. Probing Zeolites by Vibrational Spectroscopies. *Chem. Soc. Rev.* **2015**, *44*, 7262–7341.

(46) Hughes, T. R.; White, H. M. A Study of the Surface Structure of Decationized Y Zeolite by Quantitative Infrared Spectroscopy. *Phys. Chem.* **1967**, *71*, 2192–2201.

(47) Corma, A.; Fornés, V. On the 3625 Cm-1 OH Stretching Band in HNa-Y Zeolites. *Zeolites* **1983**, *3*, 197–198.

(48) Joseph, J.; Jemmis, E. D. Red-, Blue-, or No-Shift in Hydrogen Bonds: A Unified Explanation. *J. Am. Chem. Soc.* **2007**, *129*, 4620–4632.

(49) Parry, E. P. An Infrared Study of Pyridine Adsorbed on Acidic Solids. Characterization of Surface Acidity. *J. Catal.* **1963**, *2* (5), 371–379. https://doi.org/10.1016/0021-9517(63)90102-7.

(50) John Wiley & Sons, I. S. SpectraBase Compound ID=IDgOu9LX6IZ SpectraBase Spectrum ID=4F262NjKxTp.

(51) John Wiley & Sons, I. S. SpectraBase Compound ID=89V8gJyNCOb SpectraBase Spectrum ID=Fulhh0stkzb.

(52) Kumar, G.; Bossert, H.; McDonald, D.; Chatzidimitriou, A.; Ardagh, M. A.; Pang, Y.; Lee, C. S.; Tsapatsis, M.; Abdelrahman, O. A.; Dauenhauer, P. J. Catalysis-in-a-Box: Robotic Screening of Catalytic Materials in the Time of COVID-19 and Beyond. *Matter* **2020**, *3*, 805–823.

(53) Maduskar, S.; Teixeira, A. R.; Paulsen, A. D.; Krumm, C.; Mountziaris; Fan, W.; Dauenhauer, P. J.; Mountziaris, T. J.; Fan, W.; Dauenhauer, P. J. Quantitative Carbon Detector (QCD) for Calibration-Free, High-Resolution Characterization of Complex Mixtures. *Lab Chip* **2015**, *15* (2), 440–447. https://doi.org/10.1039/C4LC01180E.

(54) William E. Wallace, director. "Mass Spectra." *NIST Mass Spectrom. Data Cent.*

(55) IZA Database. Accessed Feb, 2021.

(56) Treacy, M. M. J.; Foster, M. D. Packing Sticky Hard Spheres into Rigid Zeolite Frameworks. *Microporous Mesoporous Mater.* **2009**, *118* (1–3), 106–114. https://doi.org/10.1016/j.micromeso.2008.08.039.

(57) Zhang, J.; Zhao, Y.; Feng, X.; Pan, M.; Zhao, J.; Ji, W.; Au, C. T. Na2HPO4-Modified NaY Nanocrystallites: Efficient Catalyst for Acrylic Acid Production through Lactic Acid Dehydration. *Catal. Sci. Technol.* **2014**, *4*, 1376–1385.

(58) Hattori, H.; Ono, Y. *Catalysts and Catalysis for Acid-Base Reactions*; Elsevier Inc., 2018; Vol.

1. https://doi.org/10.1016/B978-0-12-811631-9.00004-1.

(59)   Yan, B.; Tao, L. Z.; Liang, Y.; Xu, B. Q. Sustainable Production of Acrylic Acid: Catalytic Performance of Hydroxyapatites for Gas-Phase Dehydration of Lactic Acid. *ACS Catal.* **2014**, *4*, 1931–1943.

(60)   Wang, B.; Li, C.; Zhu, Q.; Tan, T. The Effect of K2HPO4and Al2(SO4)3modified MCM-41 on the Dehydration of Methyl Lactate to Acrylic Acid. *RSC Adv.* **2014**, *4*, 45679–45686.

(61)   Mok, W. S. L.; Antal, M. J.; Jones, M. Formation of Acrylic Acid from Lactic Acid in Supercritical Water. *J. Org. Chem.* **1989**, *54*, 4596–4602.